Piecewise-linear (PWL) canard dynamics: Simplifying singular perturbation theory in the canard regime using piecewise-linear systems

Mathieu Desroches, Soledad Fernández-García, Martin Krupa, Rafel Prohens, Antonio Teruel

Piecewise-linear (PWL) canard dynamics

Simplifying singular perturbation theory in the canard regime using piecewise-linear systems

Mathieu Desroches, Soledad Fernández-García, Martin Krupa, Rafel Prohens, and Antonio E. Teruel

Abstract In this chapter we gather recent results on piecewise-linear (PWL) slow-fast dynamical systems in the canard regime. By focusing on minimal systems in $\mathbb{R}^2$ (one slow and one fast variables) and $\mathbb{R}^3$ (two slow and one fast variables), we prove the existence of (maximal) canard solutions and show that the main salient features from smooth systems is preserved. We also highlight how the PWL setup carries a level of simplification of singular perturbation theory in the canard regime, which makes it more amenable to present it to various audiences at an introductory level. Finally, we present a PWL version of Fenichel theorems about slow manifolds, which are valid in the normally hyperbolic regime and in any dimension, which also offers a simplified framework for such persistence results.

Key words: piecewise-linear systems, singularly perturbed systems, canard solution, slow manifolds

1 Introduction

Singularly perturbed systems of ordinary differential equations are written in standard form as

M. Dessroches and M. Krupa
MathNeuro Team, Inria Sophia Antipolis Research Centre 2004 route des Lucioles BP93, 06902 Sophia Antipolis cedex, France, e-mail: mathieu.desroches@inria.fr

S. Fernández-García
Departamento EDAN, University of Sevilla, Facultad de Matemáticas, C/ Tarfia, s/n., 41012 Sevilla, Spain.

R. Prohens and A. E. Teruel
Departament de Matemàtiques i Informàtica, Universitat de les Illes Balears, Carretera de Valldemossa km. 7.5. 07122, Palma de Mallorca, Spain.

$$\varepsilon\dot{\mathbf{x}} = \varepsilon\frac{d\mathbf{x}}{dt} = \mathbf{f}(\mathbf{x},\mathbf{y},\varepsilon), \quad \dot{\mathbf{y}} = \frac{d\mathbf{y}}{dt} = \mathbf{g}(\mathbf{x},\mathbf{y},\varepsilon), \tag{1}$$

where $(\mathbf{x},\mathbf{y}) \in \mathbb{R}^q \times \mathbb{R}^s$ are the state variables, $\mathbf{f}$ and $\mathbf{g}$ are sufficiently smooth functions and $0 < \varepsilon \ll 1$ is a small parameter. From the expression above, the coordinates of $\mathbf{x}$ and $\mathbf{y}$ evolve with a different speed, provided that ε is small enough. Thus, the coordinates of $\mathbf{x}$ are called fast variables, while the coordinates of $\mathbf{y}$ are called slow variables. The time variable t is referred to as the slow time.

Changing the time t to the fast time $\tau = t/\varepsilon$, system (1) is written as

$$\mathbf{x}' = \frac{d\mathbf{x}}{d\tau} = \mathbf{f}(\mathbf{x},\mathbf{y},\varepsilon), \quad \mathbf{y}' = \frac{d\mathbf{y}}{d\tau} = \varepsilon\mathbf{g}(\mathbf{x},\mathbf{y},\varepsilon). \tag{2}$$

Systems (1) and (2) are differentiably equivalent and their phase portraits are the same. Both dynamics exhibit an slow-fast explicit splitting. In this setting, systems (1) and (2) are called slow-fast systems. Often, system (1) is referred to as the slow system whereas system (2) is called the fast system.

Fenichel's geometric theory [11] allows to analyse the dynamics of the perturbed system (1) by combining the behaviour of the singular orbits, corresponding to the limiting cases given by $\varepsilon = 0$. In particular, by setting $\varepsilon = 0$ in equations (1) and (2), we get respectively the differential algebraic equation (DAE)

$$\mathbf{0} = \mathbf{f}(\mathbf{x},\mathbf{y},0), \quad \dot{\mathbf{y}} = \mathbf{g}(\mathbf{x},\mathbf{y},0), \tag{3}$$

typically referred to as the slow subsystem or reduced problem, and the fast subsystem or layer problem

$$\mathbf{x}' = \mathbf{f}(\mathbf{x},\mathbf{y},0), \quad \mathbf{y}' = \mathbf{0}. \tag{4}$$

The reduced problem consists of an s-dimensional vector field defined on the critical manifold $\mathscr{S} = \{(\mathbf{x},\mathbf{y}) \in \mathbb{R}^{q+s} \,|\, \mathbf{f}(\mathbf{x},\mathbf{y},0) = \mathbf{0}\}$, which is assumed to be an s-dimensional manifold. Regarding the layer problem, its dynamical behaviour takes place along q-dimensional fibers which are formed by considering $\mathbf{y}$ constant. Hence, both limiting problems have dimension lower than that of the perturbed system. Moreover, the critical manifold $\mathscr{S}$ plays a key role in both limiting problems : it is the phase space of the reduced systems and it corresponds to singular points of the layer problem. A singular point $(\mathbf{x}_0,\mathbf{y}_0) \in \mathscr{S}$ is said to be normally hyperbolic if the eigenvalues of the Jacobian matrix $\mathbf{f}_\mathbf{x}(\mathbf{x}_0,\mathbf{y}_0,0)$ have nonzero real part.

The flow of the reduced problem can be analysed by differentiating the equation of the critical manifold $\mathscr{S}$ with respect to the slow time t, which yields

$$\dot{\mathbf{x}} = \pm\mathbf{f}_\mathbf{x}^{-1}\mathbf{f}_\mathbf{y}\mathbf{g}(\mathbf{x},\mathbf{y},0), \quad \dot{\mathbf{y}} = \mathbf{g}(\mathbf{x},\mathbf{y},0), \tag{5}$$

where $\mathbf{f}_\mathbf{x}$ (resp. $\mathbf{f}_\mathbf{y}$) denotes the differential of $\mathbf{f}$ with respect to the fast (resp. slow) variables. Then, system (5) is clearly singular at non-hyperbolic points (in particular in the fold set $\mathscr{F}$), which can be remedied by rescaling time by a factor $\pm\det(\mathbf{f}_\mathbf{x})$ (owing to Kramer's rule). This brings the so-called *desingularised reduced system* (DRS)

$$\dot{\mathbf{x}} = \mathbf{f}_\mathbf{y}\mathbf{g}(\mathbf{x},\mathbf{y},0), \quad \dot{\mathbf{y}} = \pm\det(\mathbf{f}_\mathbf{x})\mathbf{g}(\mathbf{x},\mathbf{y},0), \tag{6}$$

which by construction is regular everywhere including in the fold set, and has the same orbits as the reduced system with simply an opposite direction along the repelling sheet $\mathscr{S}^r$ of the critical manifold.

Consider $\mathscr{S}_0 \subset \mathscr{S}$ a compact set such that every point in $\mathscr{S}_0$ is a normally hyperbolic singular point. From Fenichel's Theorems [11], the submanifold $\mathscr{S}_0$ persists as a locally invariant slow manifold $\mathscr{S}_\varepsilon$, of the perturbed system (1) for every small enough ε. Moreover, the restriction of the flow of the perturbed system (1) to the slow manifold $\mathscr{S}_\varepsilon$ is a small smooth perturbation of the flow of the reduced problem (3). Fenichel also proved that there exists an invariant foliation with basis $\mathscr{S}_\varepsilon$ with the dynamics along each fiber being a small smooth perturbation of the flow of the layer problem. See also Jones, [18], for a survey on geometric singular perturbation theory (GSPT).

In Section 2, we show that these results apply when the assumption of smoothness of the vector field is relaxed. In particular, we state a variant of Fenichel theorem in the context of piecewise-linear slow-fast systems, with slow dynamics given by a linear differential equation and a critical manifold given by the graph of a piecewise linear (PWL) function. A key aspect of this result is that, due to the PWL setting, explicit formulation are obtained for canonical linear slow manifolds.

Following Fenichel results, under normal hyperbolicity conditions, orbits of the perturbed system (1) are composed by slow and fast segments. The former ones evolving close to the flow defined over the slow manifold, while the latter ones are following the flow defined over the fast fibers. A general question is: *what does remain of this dynamical behaviour when normal hyperbolicity is lost?* in particular, at points $(\mathbf{x}_0, \mathbf{y}_0) \in \mathscr{S}$ where the critical manifold is folded, that is, at which the determinant of the Jacobian matrix $\mathbf{f}_\mathbf{x}(\mathbf{x}_0, \mathbf{y}_0, 0)$ vanishes. Typically, when the critical manifold $\mathscr{S}$ folds, then the fold set (a point or a curve in the most examples treated here) separates branches with different stability properties. Consequently, attracting (resp. repelling or saddle-type) branches of $\mathscr{S}$ perturb to attracting (resp. repelling or saddle-type) slow manifolds $\mathscr{S}^a_\varepsilon$ (resp. $\mathscr{S}^r_\varepsilon$ or $\mathscr{S}^s_\varepsilon$). Then, in the vicinity of the fold set of $\mathscr{S}$, conditions can be obtained for slow manifolds with different stability to connect, hence allowing for the existence of orbits which closely follow an attracting slow manifold $\mathscr{S}^a_\varepsilon$, pass close to fold set of $\mathscr{S}$, and subsequently follow closely a repelling slow manifold, $\mathscr{S}^r_\varepsilon$. These orbits are called *canards* and they play a crucial role in explaining complicated slow-fast dynamics organising the transition between stationary and relaxation regimes in planar systems (see Section 3) or the transition between different oscillatory regimes (see Sections 4).

The aforementioned conditions for slow manifolds with different stability to connect, are obtained by the linear analysis of certain equilibria of the DRS (6), namely those lying on the fold set $\mathscr{F}$ and hence satisfying $\det(\mathbf{f}_\mathbf{x}) = 0$. Such equilibria are called *folded singularities* and they appear due to the (singular) time rescaling which transforms (5) into (6). Note that folded singularities are not equilibria of the slow flow. Therefore, depending on the local behaviour in a neighbourhood of the folded singularity, trajectories starting on $\mathscr{S}^a$ may cross them in finite time and continue flowing along $\mathscr{S}^r$, which is a singular canard behaviour. These singular canards al-

low for the existence of canard solutions in the original system for small enough $\varepsilon > 0$; see Section 4 for details.

Seminal and classical papers on canards in planar systems are those of Benoît et al. [3], Dumortier and Roussarie [10], and Krupa and Szmolyan [21, 22]. Regarding canards in higher- dimensional systems with (at least) two slow and one fast variables, see [2, 4, 28]; a recent survey can be found in [8].

Singularly perturbed PWL systems exhibiting canard dynamics are considered in Section 3 and 4 in the two and three dimensional cases with two slow variables, respectively; a brief summary of initial results on an example of three-dimensional case with two fast variables (in the context of *bursting*) is briefly mentioned in the conclusion section. Through these examples one can conclude that the PWL framework is able to reproduce all salient dynamical features present in the smooth case, both qualitatively and quantitatively, while allowing for a substantial level of simplification. What is more, these examples also suggest elements that naturally appear in the PWL setting and help revisiting unsettled questions from the smooth case. To paraphrase M. Diener in [9], the natural biotope of canards is that of PWL vector field. At least, it seemingly appears as the simplest environment in which one can understand the essence of canard dynamics while dropping all unnecessary refinements.

2 Canonical Fenichel slow manifolds

Under suitable conditions (most importantly, normal hyperbolicity of the unperturbed manifold), Fenichel theory guarantees the existence of slow manifolds perturbing from the critical manifold, when $\varepsilon > 0$ is sufficiently small. These slow manifolds are locally invariant by the flow of the smooth system (1); however, just like centre manifolds, Fenichel slow manifolds are not necessarily unique. A proof of these results can be found in [18, 19].

In this section a version of Fenichel Theorem is stated in the context of slow-fast PWL systems. In particular, we consider slow-fast PWL systems with s slow and 1 fast variables, of the form

$$\begin{cases} x' = -|x| + \mathbf{e}_1^T \mathbf{y}, \\ \mathbf{y}' = \varepsilon(\mathbf{a}x + A\mathbf{y} + \mathbf{b}), \end{cases} \tag{7}$$

where $A = (a_{ij})_{1\leq i,j\leq s}$ is an $s \times s$ real matrix, $\mathbf{e}_1$ is the first element of the canonical basis in $\mathbb{R}^s$, $\mathbf{a} = (a_i)_{1\leq i,j\leq s}^T$ and $\mathbf{b} = (b_i)_{1\leq i,j\leq s}^T$ are vectors in $\mathbb{R}^s$, and the superscript T stands for the transposed vector. Note that system (7) is linear on each side of the switching manifold $\{x = 0\}$.

The critical manifold associated with system (7) is $\mathscr{S} = \{(x, \mathbf{y}) : \ |x| = \mathbf{e}_1^T \mathbf{y}\}$. It is formed by the union of the two s-dimensional manifolds

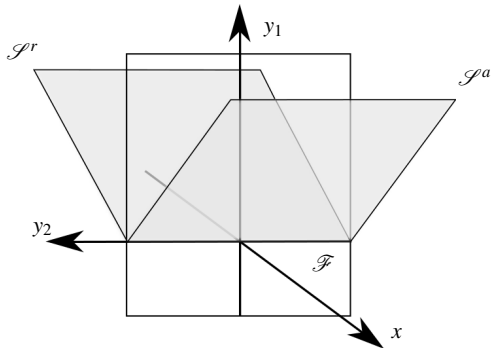

Fig. 1 (Color) 3D representation of the critical manifold $\mathscr{S}$ of system (7). From the fast subsystem, it can be noticed that the attracting branch of the critical manifold $\mathscr{S}^a$ corresponds to the half plane contained in the half space $\{x > 0\}$, the repelling branch of the critical manifold $\mathscr{S}^r$ corresponds to the half plane contained in the half space $\{x < 0\}$, and the fold manifold $\mathscr{F}$ corresponds to the segment contained in the switching manifold $\{x = 0\}$.

$$\begin{aligned} \mathscr{S}^a &= \{(x,\mathbf{y}) : x > 0, x = \mathbf{e}_1^T\mathbf{y}\}, \\ \mathscr{S}^r &= \{(x,\mathbf{y}) : x < 0, x = -\mathbf{e}_1^T\mathbf{y}\}, \end{aligned} \tag{8}$$

connected by the $(s-1)$-dimensional fold set $\mathscr{F} = \{(0,\mathbf{y}) : \mathbf{e}_1^T\mathbf{y} = 0\}$, see Figure 1 for a three-dimensional representation.

The critical manifold $\mathscr{S}$ is normally hyperbolic, except in the fold set $\mathscr{F}$; the branch $\mathscr{S}^a$ is attracting and the branch $\mathscr{S}^r$ is repelling. Since the vector field defined by (7) is smooth in each of the half–spaces $\{x > 0\}$ and $\{x < 0\}$ (it is linear), Fenichel theory applies locally to each of these systems. Therefore compact submanifolds of the two branches $\mathscr{S}^a$ and $\mathscr{S}^r$ persist under the flow of system (7) as locally invariant slow manifolds for small enough $\varepsilon > 0$.

A strong gain of using the PWL setting is that one can prove the persistence of the entire manifolds $\mathscr{S}^a$ and $\mathscr{S}^r$ as locally invariant slow manifolds, and not just compact submanifolds; we denote these slow manifolds by $\mathscr{S}^a_\varepsilon$ and $\mathscr{S}^r_\varepsilon$, respectively. Since these manifolds are contained in the half-spaces where the system is linear, their dynamical behaviour can be deduced from the spectra of the corresponding matrices, that is,

$$B^+_\varepsilon = \begin{pmatrix} -1 & \mathbf{e}_1^T \\ \varepsilon\mathbf{a} & \varepsilon A \end{pmatrix} \quad \text{and} \quad B^-_\varepsilon = \begin{pmatrix} 1 & \mathbf{e}_1^T \\ \varepsilon\mathbf{a} & \varepsilon A \end{pmatrix}, \tag{9}$$

respectively.

Following [27], we can obtain explicit equations for these slow manifolds by proceeding as follows. The spectrum of $B^\pm_\varepsilon$ decomposes into two parts: one composed by a real eigenvalue of $O(1)$ and the other one formed by s eigenvalues (counted with multiplicity) of $O(\varepsilon)$. We consider the spectra of both B^+_ε and B^-_ε simultane-

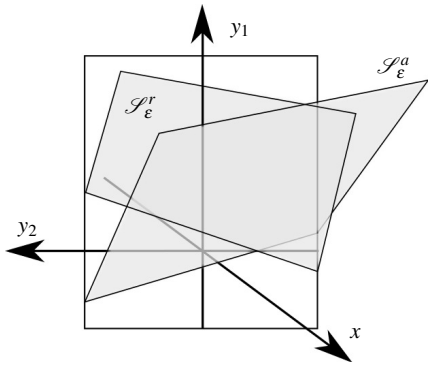

Fig. 2 (Color) 3D representation of the attracting slow manifold $\mathscr{S}_\varepsilon^a$ and the repelling slow manifold $\mathscr{S}_\varepsilon^r$ of system (7).

ously (see [27, Lemma 3]) and write the eigenvalues as

$$\lambda_1^{\pm} = \mp 1 + O(\varepsilon) \quad \text{and} \quad \lambda_k^{\pm} = \beta_k^{\pm}\varepsilon + O(\varepsilon^2),\ k = 2,\dots,s+1.$$

The eigenvalue $\lambda_1^{\pm}$ is responsible for the fast dynamics whereas the s eigenvalues $\lambda_k^{\pm}$ are responsible for the slow dynamics. Consequently, for small enough $\varepsilon > 0$ the slow dynamics in the half–space $\{x > 0\}$ is restricted to the half-hyperplane defined by the generalized eigenvectors associated with the eigenvalues $\{\lambda_k^+\}_{k=2}^{s+1}$. From [27, Lemma 5], we conclude that the slow manifold in $\{x \geq 0\}$ is given by the half–hyperplane

$$\mathscr{S}_\varepsilon^a = \left\{ (x,\mathbf{y}) \in \mathbb{R}^n :\ x \geq 0,\ x = \mathbf{e}_1^T (\varepsilon A - \lambda_1^+ I)^{-1} \left(\frac{\varepsilon}{\lambda_1^+}\mathbf{b} + \mathbf{y} \right) \right\}, \qquad (10)$$

see [27] for more details. As mentioned above, the fast dynamics in $\{x > 0\}$ is organized by the fast negative eigenvalue λ_1^+. Therefore, $\mathscr{S}_\varepsilon^a$ is an attracting slow manifold.

Similarly, the slow dynamics in the half–space $\{x < 0\}$ is restricted to the half-hyperplane defined by the generalized eigenvectors associated with the eigenvalues $\{\lambda_k^-\}_{k=2}^{s+1}$ and given by

$$\mathscr{S}_\varepsilon^r = \left\{ (x,\mathbf{y}) \in \mathbb{R}^n :\ x \leq 0,\ x = \mathbf{e}_1^T (\varepsilon A - \lambda_1^- I)^{-1} \left(\frac{\varepsilon}{\lambda_1^-}\mathbf{b} + \mathbf{y} \right) \right\}. \qquad (11)$$

In this case, the fast dynamics is organized by the positive eigenvalue λ_1^-, and hence, $\mathscr{S}_\varepsilon^r$ is a repelling slow manifold.

A 3-dimensional representation of the slow manifolds is shown in Figure 2. The slow manifolds in the 3-dimensional PWL system have been explicitly computed in [26].

One can prove that $\mathscr{S}_\varepsilon^{a,r}$ are Fenichel slow manifolds and that they possess similar properties as Fenichel slow manifolds in smooth systems. Therefore, one can extend Fenichel's theorem to the case of PWL system, as stated below; see [26, 27] for a proof of this result.

Theorem 1 (Fenichel theorem for PWL systems). *For $\varepsilon > 0$ and sufficiently small, the manifolds $\mathscr{S}_\varepsilon^{a,r}$ satisfy the following :*

a) $\mathscr{S}_\varepsilon^{a,r}$ is locally invariant under the flow of system (7).
b) The restriction of the flow of system (7) *to $\mathscr{S}_\varepsilon^{a,r}$ is a regular perturbation of the flow of the reduced problem defined on the critical manifold $\mathscr{S}$.*
c) $\mathscr{S}_\varepsilon^{r}$ is a repelling slow manifold and $\mathscr{S}_\varepsilon^{a}$ is an attracting slow manifold.
d) Given a compact subset $\hat{\mathscr{S}}^a$ (resp. $\hat{\mathscr{S}}^r$) of $\mathscr{S}^a$ (resp. $\mathscr{S}^r$), there exists a compact subset $\hat{\mathscr{S}}_\varepsilon^a$ (resp. $\hat{\mathscr{S}}_\varepsilon^r$) of the slow manifold $\mathscr{S}_\varepsilon^a$ (resp. $\mathscr{S}_\varepsilon^r$) which is diffeomorphic to $\hat{\mathscr{S}}^a$ (resp. $\hat{\mathscr{S}}^r$) such that $d_H(\hat{\mathscr{S}}_\varepsilon^a, \hat{\mathscr{S}}^a) = O(\varepsilon)$ (resp. $d_H(\hat{\mathscr{S}}_\varepsilon^r, \hat{\mathscr{S}}^r) = O(\varepsilon)$), where d_H denotes the Hausdorff distance.

2.1 Simplification in the PWL setting

Contrary to the original Fenichel's Theorem, Theorem 1 offers an explicit expression for $\mathscr{S}_\varepsilon^{a,r}$. These slow manifolds are *canonical* in the sense that they are uniquely defined, they are the only linear slow manifolds as well as the only ones on which the dynamics has no influence from the fast eigenvalues. In other words, solutions on any other invariant manifold contain a component of the form $e^{t\,\lambda_1^{\pm}}$. Hence, as soon as this component becomes dominant, the orbit is not part of a slow manifold any more. That is why all other (nonlinear) slow manifolds are only locally invariant. Hence, $\mathscr{S}_\varepsilon^{a,r}$ are canonically slow and, to a certain extent, they are the "best" Fenichel manifolds that one can hope for in any singularly perturbed system.
This is a major difference with the smooth case and the existence of such unique linear slow manifolds offers a key advantage. Indeed, their explicit equations (10) and (11) are very useful to locate maximal canard solutions, which are specific orbits passing from the attracting slow manifold $\mathscr{S}_\varepsilon^a$ to the repelling slow manifold $\mathscr{S}_\varepsilon^r$; see Sections 3 and 4 below and [6, 26, 27] for details.

2.2 A necessary perturbation to obtain canard dynamics

Within the PWL setup presented in the previous section, one can entirely reproduce relaxation oscillations that are typical in van der Pol (VDP) type systems. One only needs to consider in place of the cubic critical manifold of the VDP system, the graph of a piecewise-linear function with three pieces; in other words, one approximates the quadratic fold points of the VDP critical manifold by corners. Then, relax-

ation oscillations can be generated and their properties are perfectly similar to those generated by the VDP system. Moreover, when the slow nullcline is non-vertical, then the resulting PWL caricature of the VDP system is typically called the McKean model and it has been thoroughly studied in the relaxation regime since the early 1970s [23]. In fact, the McKean model is a caricature of the so-called FitzHugh-Nagumo model, which amounts to the VDP system where the slow nullcline is not vertical and gives a simple phenomenological model of action potential generation in neurons [15, 25]. However, when attempting to reproduce canard dynamics from the VDP system, approximating the quadratic fold points of the associated critical manifold by corners is not sufficient and a refinement is required in order to recover the slow passage from the attracting side to the repelling side of the critical manifold, as we explain below. Indeed, since the late 1990s with the work of Arima et al. [1], it is known that three linearity zones are needed to approximate locally the van der Pol system in order to get canard dynamics. In order words, the PWL critical manifold must locally have three segments in order to correctly approximate the quadratic critical manifold of the van der Pol system and open the possibility for canard cycles to appear.

We now consider the following slow-fast PWL systems,

$$\begin{cases} x' = -|x|_{\boldsymbol{\delta}} + \mathbf{e}_1^T \mathbf{y}, \\ \mathbf{y}' = \varepsilon(\mathbf{a}x + A\mathbf{y} + \mathbf{b}), \end{cases} \tag{12}$$

where the generalized absolute value function $|x|_{\boldsymbol{\delta}}$ is defined as follows

$$|x|_{\boldsymbol{\delta}} = \begin{cases} -x-(m+1)\delta^- & x \leq -\delta^-, \\ mx & -\delta^- \leq x \leq \delta^+, \\ x+(m-1)\delta^+ & \delta^+ \leq x, \end{cases}$$

and $\boldsymbol{\delta} = (\delta^-, m, \delta^+)$ is a continuous function of ε such that $\boldsymbol{\delta}(0) = \mathbf{0}$.

Since the function $|x|_{\mathbf{0}}$ coincides with the absolute value function, the layer and the reduced problems associated with system (12) are identical to those associated with system (7). Thus, the critical manifold $\mathscr{S}$ also coincides with that defined for system (7).

For $\varepsilon > 0$ small enough, system (12) is a slow-fast PWL system, locally linear in the three closed regions $\{x \leq -\delta^-\}$, $\{-\delta^- \leq x \leq \delta^+\}$, and $\{x \geq \delta^+\}$, which we will refer to from now on as the left, central and right zones, respectively. Therefore, the dynamics of system (12) in the lateral regions can be deduced from the spectra of the matrices (9), whereas in the central region it is deduced from the spectrum of the matrix

$$B_\varepsilon^0 = \begin{pmatrix} m & \mathbf{e}_1^T \\ \varepsilon\mathbf{a} & \varepsilon A \end{pmatrix}.$$

As previously shown, the slow behaviour in the lateral regions is reduced to linear manifolds, which are defined by the eigenvectors associated with the slow eigenvalues. Therefore, the canonical slow manifolds in the lateral regions are parallel to those defined in (10) and (11), namely we have

$$\mathscr{S}_\varepsilon^a = \left\{ (x,\mathbf{y}) \in \mathbb{R}^n :\ x \geq \delta^+,\ x = \mathbf{e}_1^T (\varepsilon A - \lambda_1^+ I)^{-1} \left(\frac{\varepsilon}{\lambda_1^+}\mathbf{b} + \mathbf{y} \right) - \frac{(1-m)\delta^+}{\lambda_1^+} \right\}, \tag{13}$$

$$\mathscr{S}_\varepsilon^r = \left\{ (x,\mathbf{y}) \in \mathbb{R}^n :\ x \leq -\delta^-,\ x = \mathbf{e}_1^T (\varepsilon A - \lambda_1^- I)^{-1} \left(\frac{\varepsilon}{\lambda_1^-}\mathbf{b} + \mathbf{y} \right) - \frac{(1+m)\delta^-}{\lambda_1^-} \right\}.$$

Note that the eigenvalue λ_1^+ is the fast one in the right zone $\{x \geq \delta^+\}$ and the eigenvalue λ_1^- is the fast one in the left zone $\{x \leq -\delta^-\}$.

Regarding the dynamics in the central region, every non zero eigenvalue of B_ε^0 is $O(\varepsilon^\alpha)$, $\alpha \in \mathbb{R}$. Hence, in order for the flight time in the central region not to diverge to infinity as $\varepsilon \to 0$, we assume that δ^+ and δ^- have greater order in ε than the smaller non-zero eigenvalue. Recent work has allowed to refine the results from [1] and find that the optimal of the central zone is $O(\sqrt{\varepsilon})$ [6].

Arima and co-authors have computed numerically small (so-called *headless*) canard cycles in a PWL approximation of the van der Pol system similar to (12) as well as large canard cycles (so-called *canards with head*) in a four-zone system. They gave arguments to justify the need for the three-piece critical manifold in order to make sense of a repelling slow manifold and, hence, find canards. However, they did not develop GSPT arguments proving the existence of canards in this planar context and they did not investigate three-dimensional canard systems either. This has been done more recently in [6, 13]. We summarise the results obtained in these two papers in the next two sections, which will then be entirely focused on canards in slow-fast PWL systems.

3 Canard explosion

Canard dynamics can be loosely described as a complicated mix of local passage (near non-normally hyperbolic regions of the critical manifold) and global return (or reinjection) mechanism, which allows for recurrent dynamics. Note that need not be part of recurrent dynamics. Their main feature is this local passage and it is well approximated by linear dynamics, as we shall see below. In the smooth case, the dynamics during this local passage is organised by the Weber equation, obtained (after a coupled of changes of variables) by linearising the system along the so-called "weak canard" (axis of rotation for trajectories during this local passage). It is interesting to notice that solutions to the Weber equation can be expressed in terms of parabolic cylinder functions, while in the three-dimensional PWL slow-fast system that we propose in Section 4, solutions in the central zone (approximating the local passage) are organised by invariant cylinders. In this context, canard- induced mixed-mode oscillations (MMOs, see Section 4) are a combination of small-amplitude oscillations (SAOs) near a fold curve, a passage near a repelling slow manifold and a global return that reinjects trajectory on an attracting slow manifold. In this context, the SAO part can be purely explained by linear dynamics. As al-

ready mentioned, generally speaking canards arise due to connections between an attracting slow manifold and a repelling slow manifold. These are rare events and the associated connecting orbits are called *maximal canards*; other canard solutions exist in an exponentially small neighbourhood of maximal canards. It turns out that connections between two such slow manifolds can be perfectly reproduced with PWL systems, however with an additional linearity zone in between them so as to make the passage and, hence, the connection possible. Therefore, by decomposing the dynamics of canard systems in phase space into several linear zones, one cannot only reproduce all canard phenomena —planar, three-dimensional, canard-induced MMOs, canard-induced bursting trajectories, etc..— but also properly zoom into these intricate dynamics and extract their essential features. Overall, one can say that the PWL setup offers a simpler alternative to method of "geometric desingularisation" (blow-up) studied in smooth canard systems [10, 21, 22, 28]. To this extent, the small zone in between the attracting region and the repelling region can be seen (in a loose sense) as a blow-up of the corner that one would naturally use to approximate, in the relaxation regime, the quadratic fold of the van der Pol oscillator with a PWL system.

In this section, we summarise the results published in [13] about canard cycles in planar slow-fast PWL systems. We consider the following planar version of system (12)

$$\begin{cases} x' = -|x|_{\boldsymbol{\delta}} + y, \\ y' = \varepsilon(a-x), \end{cases} \tag{14}$$

for the parameter vector

$$\boldsymbol{\delta} = \left(\frac{\varepsilon}{1-b}, -b, \frac{\varepsilon}{1+b} \right),$$

where $|b| < 2\sqrt{\varepsilon}$ and $a \in (-\varepsilon/(1-b), \varepsilon/(1+b))$.

System (14) possesses exactly one equilibrium point which is in central zone namely, $\mathbf{p}^C = (a, -ab)^T$. The topological type of this equilibrium depends on parameter b : if $b = 0$, the equilibrium point $\mathbf{p}^C$ is a center; If $b < 0$ (resp. $b > 0$) it is a stable (resp. unstable) focus.

Using the method described in Section 2, we can compute the canonical slow manifolds $\mathscr{S}_\varepsilon^{a,r}$ associated with system (14) and obtain formulas equivalent to (13), namely,

$$\begin{aligned} \mathscr{S}_\varepsilon^a &= \left\{ (x,y) \in \mathbb{R}^2 : \; x \geq \frac{\varepsilon}{1+b}, \; y = -\frac{\varepsilon}{\lambda_2^+}(x-a) + a - \varepsilon \right\}, \\ \mathscr{S}_\varepsilon^r &= \left\{ (x,y) \in \mathbb{R}^2 : \; x \leq -\frac{\varepsilon}{1-b}, \; y = -\frac{\varepsilon}{\lambda_2^-}(x-a) - a - \varepsilon \right\}. \end{aligned} \tag{15}$$

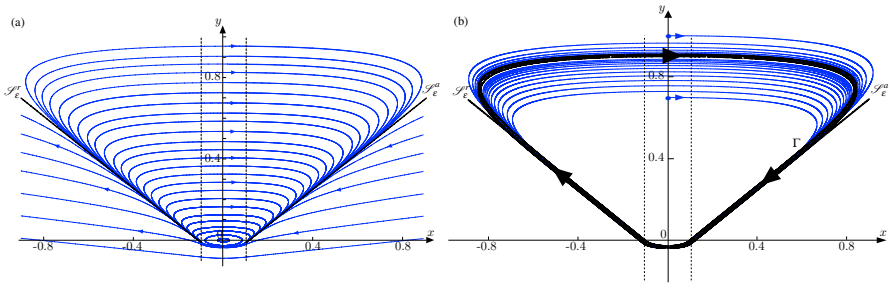

Fig. 3 (Color) (a) Continuum of canard periodic orbits bounded by the canonical slow manifolds $\mathscr{S}_\varepsilon^{a,r}$ (adapted from [13, Figure 4]). (b) Stable (headless) canard limit cycle together with the canonical slow manifolds and two trajectories approaching the canard cycle in forward time (adapted from [13, Figure 5]).

Here $\lambda_2^+ < 0$ and $\lambda_2^- > 0$ are the slow eigenvalues of the matrices B_ε^+ and B_ε^- defining the lateral linear systems, equivalent to (9).

When parameters a and b are zero, system (14) is reversible with respect to the involution $x \mapsto -x$ and the time change $t \mapsto -t$. In such a case, the slow manifolds $\mathscr{S}_\varepsilon^{a,r}$ are also images of one another under this involution and this time change. Therefore, they can connect by forming a maximal canard. The maximal canard splits the phase plane into two regions: one region contains the equilibrium point and is foliated by periodic orbits (see Figure 3), the other one is fully foliated by unbounded orbits ([13, Theorem 4.1]).

By perturbing this non-generic situation, it is possible to find a curve $a = \tilde{a}(b,\varepsilon)$ in parameter space, with Taylor series expansion at $b = 0$ given by

$$a = \tilde{a}(b,\varepsilon) = \left(\frac{\pi}{4}\sqrt{\varepsilon} + O(\varepsilon)\right) b + O(b^3), \tag{16}$$

such that, the maximal canard orbit persists ([13, Theorem 4.2 and Prop. 4.4]).

By breaking the connection that corresponds to the maximal canard, one can prove the existence of a family of canard cycles in system (14), as stated below (see [13, Theorems 4.3 and 4.5] for a proof).

Theorem 2. *For each point* $(0, y_0)$ *with* $y_0 > 0$, *there exists* $U \subset \mathbb{R}^2$ *containing* $(b,\varepsilon) = (0,0)$, *such that, for* $(b,\varepsilon) \in U \cap \{\varepsilon > 0\}$, *there exists a curve* $a(b,\varepsilon)$ *in parameter space, with the same first terms in its Taylor series expansion as* $\tilde{a}(b,\varepsilon)$, *such that system* (14) *possesses a canard cycle passing through* $(0, y_0)$. *Moreover, the family of canard limit cycles is asymptotically stable if* $b > 0$ *and unstable if* $b < 0$.

The main conclusion one can draw from the results stated so far is that canard phenomena in the PWL framework and in the classical (smooth) context have very similar features. In particular in the way they are born: a Hopf bifurcation in the smooth case, and a two-zonal Hopf-like [16, 17] bifurcation in the PWL case, which occurs when the real equilibrium point enters the central zone from either of the

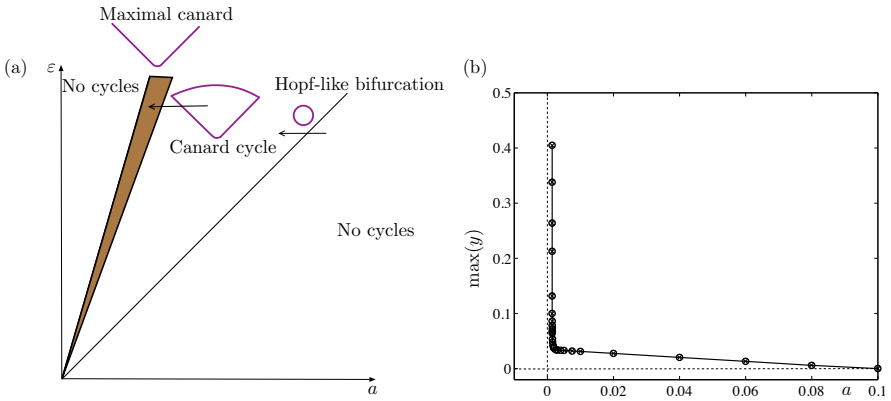

Fig. 4 (Color) (a) Bifurcation diagram for $b > 0$. Consider $\varepsilon > 0$ fixed and $a > 0$ in the rightmost sector. By decreasing a, a Hopf-like bifurcation takes place, giving rise to a small stable limit cycle. The limit cycle is growing as a decreases. When a reaches the grey-shaded region, the limit cycle becomes a canard cycle. Along the leftmost line the family of canard cycles ends at a maximal canard connection. (b) Explosive branch of limit cycles obtained by direct simulation when varying parameter a for fixed $\varepsilon = 0.1$ and $b = 0.009944$. (adapted from [13, Figure 6]).

lateral zones, by suitably moving parameter a. If we then consider $b = 2\tilde{b}\sqrt{\varepsilon}$, then we obtain the following :
– if $b > 0$, a two-zonal supercritical Hopf-like bifurcation takes place when the equilibrium enters the central zone from the right, at

$$a_H^R(b,\varepsilon) = \frac{\varepsilon}{1+b} = \varepsilon + O(\varepsilon^{3/2});$$

– if $b < 0$, a two-zonal subcritical Hopf-like bifurcation takes place when the equilibrium enters the central zone from the left, at

$$a_H^L(b,\varepsilon) = -\frac{\varepsilon}{1-b} = -\varepsilon + O(\varepsilon^{3/2}).$$

In both cases, subsequently to the Hopf-like bifurcation, the amplitude of the two-zonal limit cycle grows linearly in the two regions until it becomes a three-zonal limit cycle. Then, the third linear system affects dramatically the dynamics and the limit cycle starts to grow very rapidly, *explosively* (in terms of parameter variation), as it becomes a canard. While a increases within an exponentially small range, the amplitude of the canard cycle increases by an $O(1)$ amount until the a-value where the maximal canard occurs, $\tilde{a}(b,\varepsilon)$; see (16). Past the maximal canard, the limit cycle disappears. Figure 4 presents the bifurcation diagram corresponding to the case $b > 0$.

4 Folded singularities and their canards

Canards have been also extensively studied in systems with more than one slow and one fast variables. In particular, much is known about maximal canards in the context of three-dimensional systems with two slow variables where they appear through the presence of folded singularities, which are the equivalent to the 3D setting of canard points in VDP type systems; see [2, 4, 8, 28]. This section presents a summary of results recently published in [6] about folded singularities in 3D PWL slow-fast systems.

We consider the following PWL slow-fast system

$$\begin{cases} x' = |x|_{\boldsymbol{\delta}} - y, \\ y' = \varepsilon(p_1 x + p_2 z), \\ z' = \varepsilon p_3 \end{cases} \tag{17}$$

which then corresponds to system (12) after the change of variable $x \mapsto -x$ and with

$$\mathbf{a} = \begin{pmatrix} -p_1 \\ 0 \end{pmatrix}, \quad A = \begin{pmatrix} 0 & p_2 \\ 0 & 0 \end{pmatrix}, \quad \mathbf{b} = \begin{pmatrix} 0 \\ p_3 \end{pmatrix},$$

and $\boldsymbol{\delta} = (\delta, 0, \delta)$ for a given $\delta > 0$.

Given that system (17) can be recasted as system (12) for suitable values of matrix coefficients, we can readily apply the Fenichel analysis performed on this latter system and conclude that system (17) possesses canonical Fenichel slow manifolds $\mathscr{S}_\varepsilon^{a,r}$ given by equations (13). Slow-fast systems of this form are minimal three-dimensional systems with two slow variables displaying canard dynamics. Minimal here means that the z-dynamics is a simple slow drift. Therefore system (17) can be seen as a two-dimensional canard (VDP type) system where the parameter controlling the slow nullcline moves slowly. Such systems were first studied in [2] where conditions for connections between attracting and repelling slow manifold, that is, for maximal canards, were obtained in link with the presence of special points located along the fold curve and called folded singularities. These special points arise due to the existence of a non-normally hyperbolic set (the fold set) on the critical manifold, and they are defined in the singular limit, from the flow of the reduced system (3) (also referred to as the *slow flow*). Indeed, typical points on the fold set are jump points in the sense that the slow flow is directed towards the fold set on both sides (attracting and repelling) of such points without being defined at these points; this is because the slow flow is typically singular on the fold set. When perturbing in $\varepsilon > 0$, these points give rise to relaxation dynamics. However, one can find algebraic conditions for which points on the fold set at which the slow flow is not singular and has the same direction on both sides, hence allowing for a passage from one side of the critical manifold to the other. These special points are folded singularities (or folded equilibria) and they can be obtained as true equilibria of the DRS (6), which has the same trajectories as the slow flow but with opposite orientation on the repelling side; therefore, an equilibrium of the DRS corresponds

to a point of the reduced system at which the slow flow crosses from $\mathscr{S}^a$ to $\mathscr{S}^r$. When switching on ε with a small-enough positive value, these points give rise to canard dynamics : "true" canards if the trajectory goes from attracting to repelling and "false" (or *faux*) canards when the trajectory goes in the opposite direction. Depending on the topological type of the equilibrium point of the DRS on the fold set, one has folded equilibria of folded, saddle, focus, etc., type; see [8] for details on folded singularities and associated maximal canards.

In order to find maximal canards due to folded singularities (essentially of node and saddle type) in PWL slow-fast systems like (17), we first have to be more precise on the size of δ relative to ε so as to match an important result from the smooth case, namely that the number of maximal canards that exist for small enough ε near a folded singularity, does not depend on the specific value of ε. In particular in the folded-node scenario where multiple maximal canard can appear with both segments along $\mathscr{S}^a_\varepsilon$ and $\mathscr{S}^r_\varepsilon$ and small-amplitude oscillations (SAOs) in the fold region. The maximal number of SAO determines the type of canard solution and does not depend upon the specific value of ε. By construction, the system that we consider in the central zone is linear and the angular velocity is constant, hence the number of oscillations that trajectories make in this zone is obtained by considering the time it takes to go from one boundary of this zone to the other. This give a formula involving both δ and ε and forces a particular relationship between the two in order for this value to be independent of ε. Namely, δ has to scale like $\sqrt{\varepsilon}$; more precisely, we find that δ has to be equal to $\pi\sqrt{\varepsilon}$ for which the maximal rotation number μ is then $\dfrac{p_1\sqrt{p_1}}{|p_2 p_3|}$. This is a key result as it fixes the optimal size of the central zone in order to match results from the smooth case, that is, the optimal distance between $\mathscr{S}^a_\varepsilon$ and $\mathscr{S}^r_\varepsilon$ in order to find connections (maximal canards) entirely similar to those found in smooth slow-fast systems. We find that this optimal distance is $O(\sqrt{\varepsilon})$, which interestingly agree with the well-known result from the smooth case allowing to extend the Fenichel slow manifold up to a similar distance to the fold set before establishing conditions for them to intersect along maximal canards (using blow-up); see [4, 21, 28].

Once we have the correct scaling for the size of the central zone, we can obtain conditions for maximal canards to exist in the folded-node and in the folded-saddle cases, and verify that we have a complete similarity with these cases in smooth systems. This result is gathered in the following proposition, whose proofs are detailed in [6].

Proposition 1. *Consider system* (17) *with* $p_3 > 0$, $\delta = \pi\sqrt{\varepsilon}$ *and* ε *small enough. Assuming that different maximal canards have different flight times, the following statements hold.*

a) Maximal canards γ *are reversible orbits.*
b) If $p_1 > 0$ *and* $p_2 < 0$*, for every integer* k *with* $0 \leq k \leq [\mu]$*, where* μ *is the maximal rotation number, there exists a maximal canard* γ_k *intersecting the switching plane* $\{x = -\delta\}$ *at* $\mathbf{p}_k = (-\delta, y_k, z_k)$ *where*

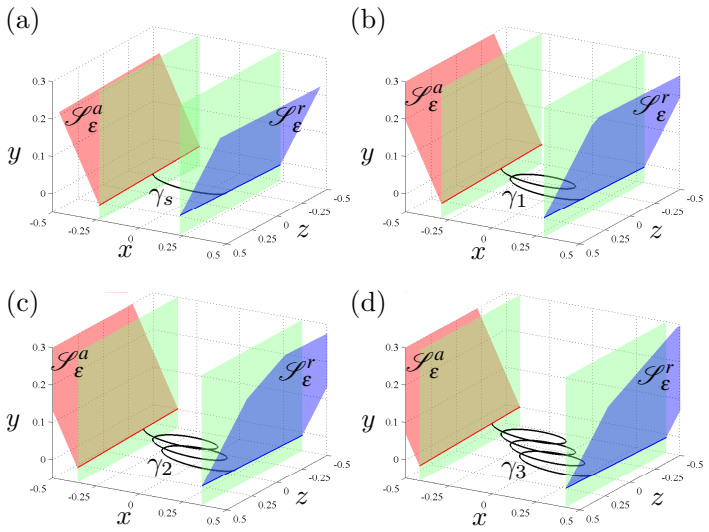

Fig. 5 (Color) Canonical slow manifolds and selected maximal canards (only central segment shown) with 0, 1, 2 and 3 SAOs in panels (a) to (d), respectively; γ_0 is then the strong canard, and γ_i the ith secondary canard ($i = 1..3$). Also shown are the switching planes at $\{x = \pm\delta\}$. [modified from [6, Figure 4.2]]

$$\begin{aligned} y_k &= -\left(\left(k+\frac{1}{2}\right)\frac{p_2 p_3}{\sqrt{p_1}} + p_1\right)\pi\varepsilon^{\frac{3}{2}} - p_2 p_3 \varepsilon^2 + O(\varepsilon^{\frac{5}{2}}), \\ z_k &= -\left(k+\frac{1}{2}\right)\frac{p_3}{\sqrt{p_1}}\pi\sqrt{\varepsilon} + O(\varepsilon). \end{aligned} \tag{18}$$

Moreover, γ_k turns k times around the weak canard γ_w.

c) *If $p_1 > 0$ and $p_2 > 0$, there exists a unique maximal canard γ_0 intersecting the switching plane at $\mathbf{p}_0 = (-\delta, y_0, z_0)$ where the coordinates y_0 and z_0 satisfy equation* (18) *with $k = 0$.*

d) *If $p_1 < 0$, there are no maximal canards.*

This result establishes the existence of maximal canards near folded singularities of system (17) that are qualitatively and quantitatively similar to those found in the smooth case [8]. In the case of a folded saddle, only one maximal canard persists for small enough $\varepsilon > 0$; near a folded node, many more do and, except for the simplest one called the *strong canard*, all other maximal canards have SAOs in the central zone and they are called *secondary canards*. In order to characterise these maximal canards, one can write a series expansion in ε. However, we can exploit the PWL structure a bit further and exhibit "selected" maximal canards by taking special values of δ (within the correct scaling), each special δ-value giving rise to one selected maximal canard for which the series expansion is exact and all terms but the very first few vanish. We show four examples of such exact maximal canard

solutions in Figure 5, for four specific values of δ selecting the strong canard and the first three secondary canards, respectively. This is one more aspect of simplification brought about by the PWL framework and that could potentially be exploited in applications.

The above results enable a full comparison between three-dimensional smooth and PWL slow-fast systems in terms of number and geometry of maximal canard solutions near both folded-node and folded-saddle singularities. However, it does not address the question of what are folded singularities in the PWL context, that is, how to define them in systems (17). This was the other main result from [6], where we introduce a strategy in order to identify the equivalent of folded singularities for three-dimensional PWL slow-fast systems with two slow variables. In brief, the main issue is to properly define the slow flow —for the $\varepsilon = 0$ limit of the fast-time system obtained from (17) by a time rescaling as described in the introduction— and exhibit conditions for singular trajectories passing from $\mathscr{S}^a$ to $\mathscr{S}^r$, that is, singular canards which all intersect at the folded singularity. The linearity zone in question is of course the central zone, which we take to be of size $\delta = O(\sqrt{\varepsilon})$ in order to keep similar properties as in the smooth case. However, this implies that $\delta \to 0$ as $\varepsilon \to 0$ and therefore the central zone shrinks to the switching planes in the singular limit, hiding information about the slow flow and, hence, about folded singularities. In order to remedy this, we artificially keep the central zone open in the singular limit and consider inside the $\varepsilon \to 0$ limit of the flow defined in there for $\varepsilon > 0$. This limiting flow allows us to find conditions, depending on p_1, p_2 and p_3, to obtain singular phase portraits entirely compatible to those of smooth singular systems near folded-node, folded-saddle and folded-saddle-node singularities, hence allowing to define the equivalent of these points in the PWL context; see [6, Section 4.4] for details.

Finally, we can also highlight the level of simplification brought by the PWL setting in this three-dimensional context. As explained above, we can "select" exact maximal canard solutions by appropriately choosing the value of δ within the correct scaling in ε. This offers almost for free maximal canards, of any type (strong or secondary), with a simple and explicit time parametrisation only depending on system parameters and ε. This is substantial gain from the smooth case, where no such explicit canards are available. We anticipate that this could be of potential in applications as maximal canards form boundaries between different activity regimes and, hence, a direct analytical access to them could help to understand and control such a dynamical system. Another gain obtained from the PWL setting in this three-dimensional case is to be able to revisit unresolved questions from the smooth case. As explained in [6], we could prove with very simple arguments that the so-called "weak canard" associated with a folded node —a solution that plays the role of rotation axis for secondary canards and whose existence as a maximal canard was not proven in smooth system— is in fact not a maximal canard. Indeed, we can compute explicitly the perturbation for small $\varepsilon > 0$ of the rotation axis defined in the central zone (in which the dynamics in restricted to the cylindrical leaves of a foliated structure) and verify that this trajectory enters the left zone at an $O(\varepsilon)$ distance to the canonical slow manifold, which makes it impossible for this trajectory to be

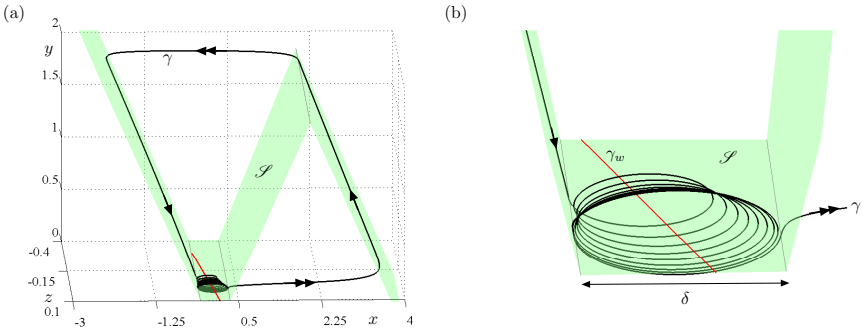

Fig. 6 (Color) Robust MMO solution γ of the three-dimensional slow-fast PWL system (17) with added linear terms in the z-equation and a fourth piece on the critical manifold, in order to ensure a global return mechanism on top of the local passage through a folded node. Also shown are the critical manifold $\mathscr{S}$ as well as the so-called weak canard (axis of rotation) γ_w. [modified from [6, Figure 5.1]]

a maximal canard since for that to happen it would need to be exponentially close to the canonical slow manifold. Given the total parallel of the canard structure in system (17) compared to smooth minimal systems for folded nodes, we conjecture that this result of the non-existence of this special trajectory as a maximal canard is also valid in the smooth context. The second question that we could revisit from the smooth concerns the possibility for SAOs near a folded-saddle singularity, which was not reported in previous studies and has been developed in the smooth case in an independent paper soon to appear in [24]. This result came naturally and easily from the PWL setting.

As an opening towards future work, we close this section by mentioning the possibility for constructing robust MMO systems by using the local dynamics previous defined and analysed, near folded nodes. It suffices to add a fourth linearity zone, immediately to the left zone of system (17), that is, adding a fourth piece to the previous critical manifold so that the new one has a corner line in the new switching plane; see Figure 6 panel (a). This is because one only needs a relaxation segment during the global return. Then, adding to the z-equation of system (17) suitable linear terms creates a global return mechanism that re-injects the trajectory near the right attracting part of the critical manifold so that it can pass again near the folded node while making SAOs. Direct simulation of this extended system indicated that one indeed obtains an MMO limit cycle whose SAOs are organised by the folded node. This is only a numerical example and we plan to prove the existence of such MMOs as well as investigate their bifurcation structure in future work.

5 Summary and perspective

In this chapter, we have presented a compendium of recent results on PWL slow-fast systems displaying canard solutions, both in the planar and the three-dimensional cases, with more general results on Fenichel slow manifolds, valid in any dimensions. Our work [6, 13, 26, 27] summarised here demonstrates that one can recover all essential results from the smooth case while gaining a substantial level of simplification in the way objects are defined and in their essential properties. This ground work has allowed us to construct minimal slow-fast systems in the PWL setup possessing maximal canard solutions by using a mix of local passage near the equivalent of the fold set and globally defined slow manifolds. These results can be used to construct complex oscillations using PWL vector fields adequately designed. We have shown the case of an MMO system with canard-induced behaviour in Figure 6. Another gain of the PWL setting is to be able to better control a given system through a more quantitative knowledge of its dynamics, which we have applied to a four-dimensional model of secreting neuron demonstrating the use of this approach [12, 14]. We have also obtained preliminary results on canard-induced bursting oscillations, that is, in the context of slow-fast systems with one slow and two fast variables. In [5], we constructed minimal PWL slow-fast systems in order to reproduce a *spike-adding canard explosion* and all salient features of square-wave bursting organised by canard solutions [7]. Surprisingly, we proved that this scenario could not be obtained in such a minimal setup with the assumption of continuity of the vector field across all linearity zones. This is a first step into investigating canard-induced complex oscillations of bursting type; ongoing and future work will involve looking at other forms of bursting with PWL systems, in particular elliptic bursting, whose understanding is a key stage towards studying canard phenomena within fast oscillations, namely, *torus canards* [20]. This case is interesting given that numerous questions are still open in the smooth case and, hence, where we believe that the PWL framework could once more prove useful with its simplification power without altering the essential dynamics.

Acknowledgments

SFG is supported by the University of Seville VPPI-US and partially supported by Proyectos de Excelencia de la Junta de Andaluca under Grant No. P12-FQM-1658 and Ministerio de Economa y Competitividad under Grant No. MTM2015-65608-P. RP and AET are supported by the Spanish Ministry of Economy and Competitiveness through project MTM2014-54275-P.

References

1. Arima, N. and Okazaki, H. and Nakano, H.: A generation mechanism of canards in a piecewise linear system. IEICE T. Fundam. Electr. **80**, 447–453 (1997)
2. Benoît, E.: Canards et enlacements. Publications Mathématiques de l'IHÉS **72**, 63–91 (1990)
3. Benoît, E. and Callot, J. L. and Diener, F. and Diener, M.: Chasse au canard. Collect. Math. **32**, 37–119 (1981)
4. Brøns, M., Krupa, M., Wechselberger, M.: Mixed mode oscillations due to the generalized canard phenomenon. Fields Institute Communications **49**, 39–63 (2006)
5. Desroches, M., Fernández-García, S., Krupa, M.: Canards in a minimal piecewise-linear square-wave burster. Chaos **26**(7), 073,111 (2016)
6. Desroches, M., Guillamon, A., Ponce, E., Prohens, R., Rodrigues, S., Teruel, A.E.: Canards, folded nodes, and mixed-mode oscillations in piecewise-linear slow-fast systems. SIAM Review **58**(4), 653–691 (2016)
7. Desroches, M., Kaper, T.J., Krupa, M.: Mixed-mode bursting oscillations: Dynamics created by a slow passage through spike-adding canard explosion in a square-wave burster. Chaos **23**(4), 046,106 (2013)
8. Desroches, M. and Guckenheimer, J.M. and Krauskopf, B. and Kuehn, C. and Osinga H. M. and Wechselberger, M.: Mixed-mode oscillations with multiple time scales. SIAM Review **54**, 211–288 (2012)
9. Diener, M.: The canard unchained or how fast/slow dynamical systems bifurcate. The Mathematical Intelligencer **6**(3), 38–49 (1984)
10. Dumortier, F. and Roussarie, R. : Canards cycles and center manifolds. Mem. Amer. Math. Soc. **557**, 1131–1162 (1996)
11. Fenichel, N.: Geometric singular perturbation theory for ordinary differential equations. J. Differential Equations **31**, 53–98 (1979)
12. Fernández-García, S., Desroches, M., Krupa, M., Clément, F.: A multiple time scale coupling of piecewise linear oscillators. application to a neuroendocrine system. SIAM J. Appl. Dyn. Syst. **14**(2), 643–673 (2015)
13. Fernández-García, S., Desroches, M., Krupa, M., Teruel, A.E.: Canard solutions in planar piecewise linear systems with three zones. Dyn. Syst. A.I.J. **31**, 173—197 (2016)
14. Fernández-García, S., Krupa, M., Clément, F.: Mixed-mode oscillations in a piecewise linear system with multiple time scale coupling. Phys. D **332**, 9–22 (2016)
15. FitzHugh, R.: Impulses and physiological states in theoretical models of nerve membrane. Biophys. J. **1**(6), 445–466 (1961)
16. Freire, E. and Ponce E. and Rodrigo. F. and Torres, F.: Bifurcation sets of continuous piecewise linear systems with two zones. J. Bifur. Chaos Appl. Sci. Engrg. **8**, 2073–2097 (1998)
17. Freire, E. and Ponce E. and Torres, F.: Hopf-like bifurcations in planar piecewise linear systems. Publ. Mat. **41**, 135–148 (1997)
18. Jones, C. K. R. T.: Geometric Singular Perturbation Theory. Springer Berlin/Heidelberg (1995)
19. Kaper, T.: Systems theory for singular perturbation problems. In: Analyzing Multiscale Phenomena Using Singular Perturbation Methods, R. E. O'Malley, Jr. and J. Cronin, editors, *Proceedings of Symposia in Applied Mathematics*, vol. 56, pp. 8–132. Amer. Math. Soc. (1999)
20. Kramer, M.A., Traub, R.D., Kopell, N.J.: New dynamics in cerebellar purkinje cells: torus canards. Physical review letters **101**(6), 068,103 (2008)
21. Krupa, M. and Szmolyan, P.: Extending geometric singular perturbation theory to nonhyperbolic points-fold and canard points in two dimensions. SIAM J. Math. Anal. **33**, 286–314 (2001)
22. Krupa, M. and Szmolyan, P.: Relaxation oscillations and canard explosion. J. Differential Equations **174**, 312–368 (2001)
23. McKean, H.P.: Nagumo's equation. Advances in Mathematics **4**(3), 209–223 (1970)
24. Mitry, J., Wechselberger, M.: Faux canards. In revision (2017)

25. Nagumo, J., Arimoto, S., Yoshizawa, S.: An active pulse transmission line simulating nerve axon. Proc. IRE **50**(10), 2061–2070 (1962)
26. Prohens, R., Teruel, A.E.: Canard trajectories in 3d piecewise linear systems. Discrete Contin. Dyn. Syst. **33**(3), 4595–4611 (2013)
27. Prohens, R., Teruel, A.E., Vich, C.: Slow-fast n-dimensional piecewise-linear differential systems. Journal of Differential Equations **260**, 1865–1892 (2016)
28. Wechselberger, M. : Existence and bifurcation of canards in $\mathbb{R}^3$ in the case of a folded node. SIAM J. Appl. Dyn. Syst. **4**, 101–139 (2005)